Electronic Supplementary Material (ESI) for Materials Advances.

Supporting Information

Naphthyl-Azine - Aggregation Induced Emission, Reversible Acidochromism, Cyanide sensing and its application in Intracellular Imaging

Sukanya Paul, Kingshuk Debsharma, Sunanda Dey, Satyajit Halder, Kuladip Jana, Chittaranjan Sinha*

Solution for Spectral Measurement

For UV-Vis and Fluorescence study, the ligand H_2L with concentration of 1x 10^{-3}(M) was prepared in DMSO. All anionic solutions of 1 x 10^{-3}(M) were arranged in CH_3CN. The Spectroscopic experiment was carried out in acetonitrile medium. A 25 μM of HL solution was prepared in2 mL CH_3CN/H_2O (99:1, v/v) (HEPES Buffer, pH 7.5) for sensing study. To this solution 2 equivalent of anions were added and the sensitivity and selectivity was checked by UV-vis and Fluorescence measurement of the probe H_2L solution. The absorption and emission path length of cell used were 1 cm. Fluorescence measurement experiments were done on excitation and emission of 12 nm x 3 nm (For HTFA vapor) and 10 nm x 10 nm (For CN^-) slit width.

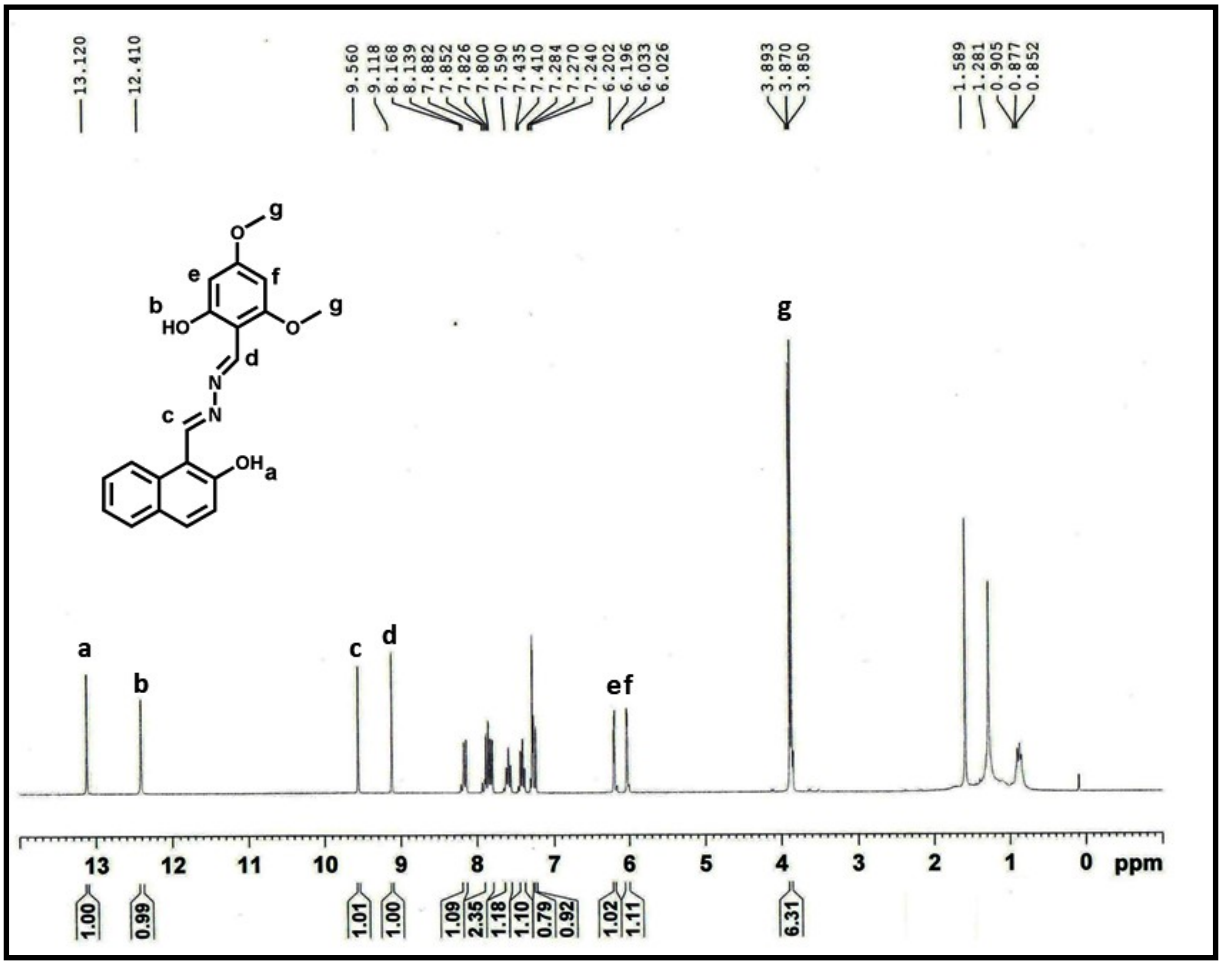

Fig. S1. ^{1}HNMR Spectra of the probe H_2L ($CDCl_3$, 300 MHz)

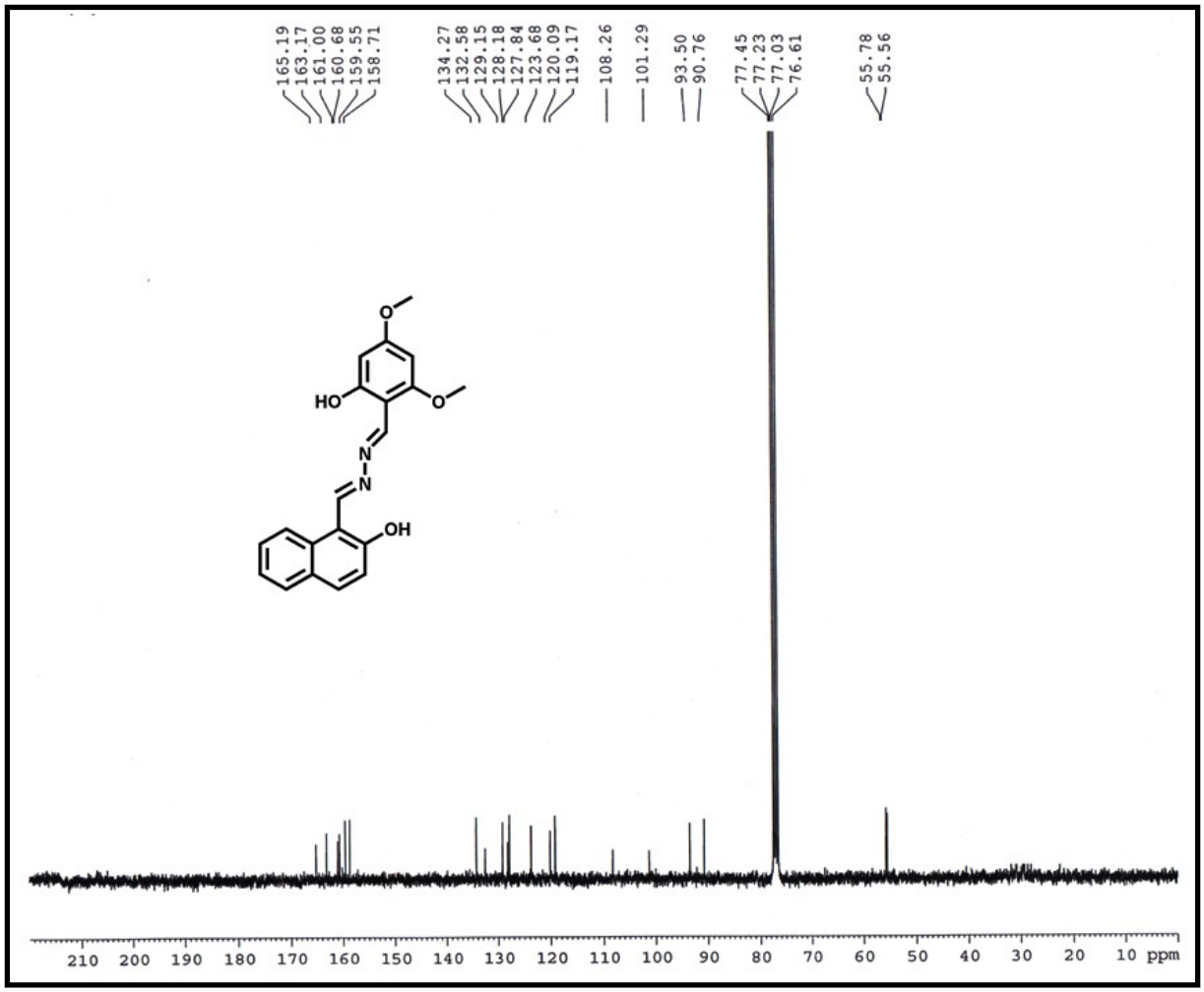

Fig. S2. ^{13}CNMR Spectrum of the probe H_2L ($CDCl_3$, 75 MHz)

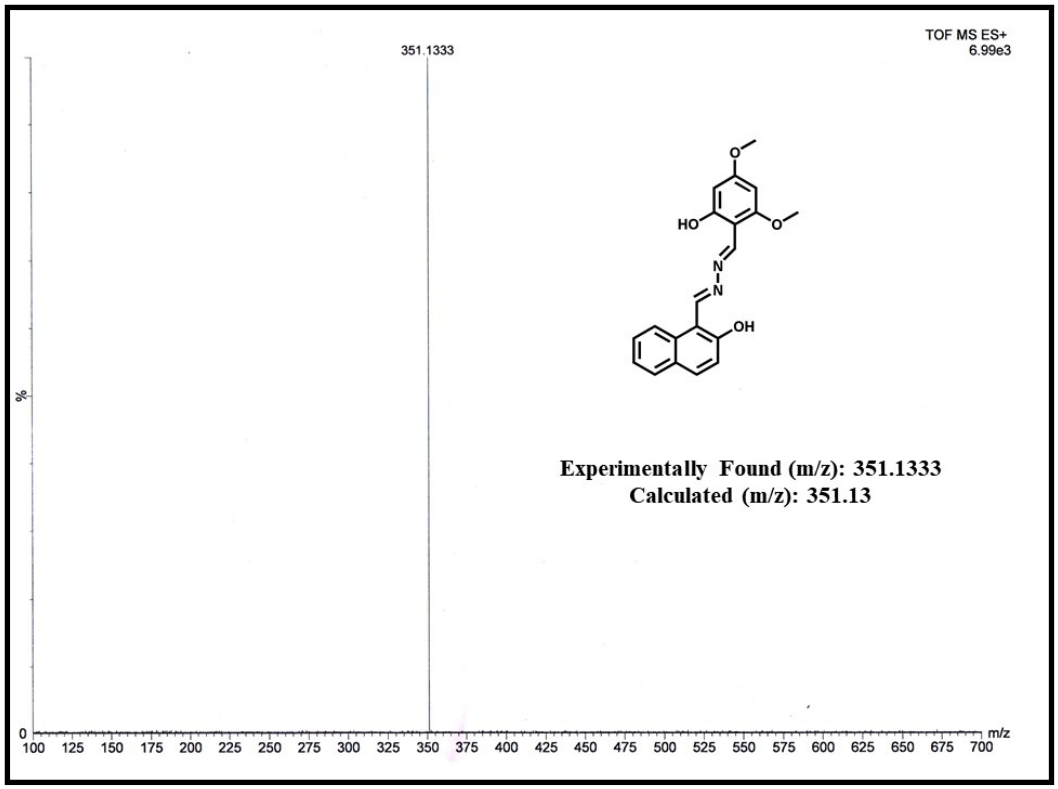

Fig.S3 ESI-MS(+) of the Ligand H_2L

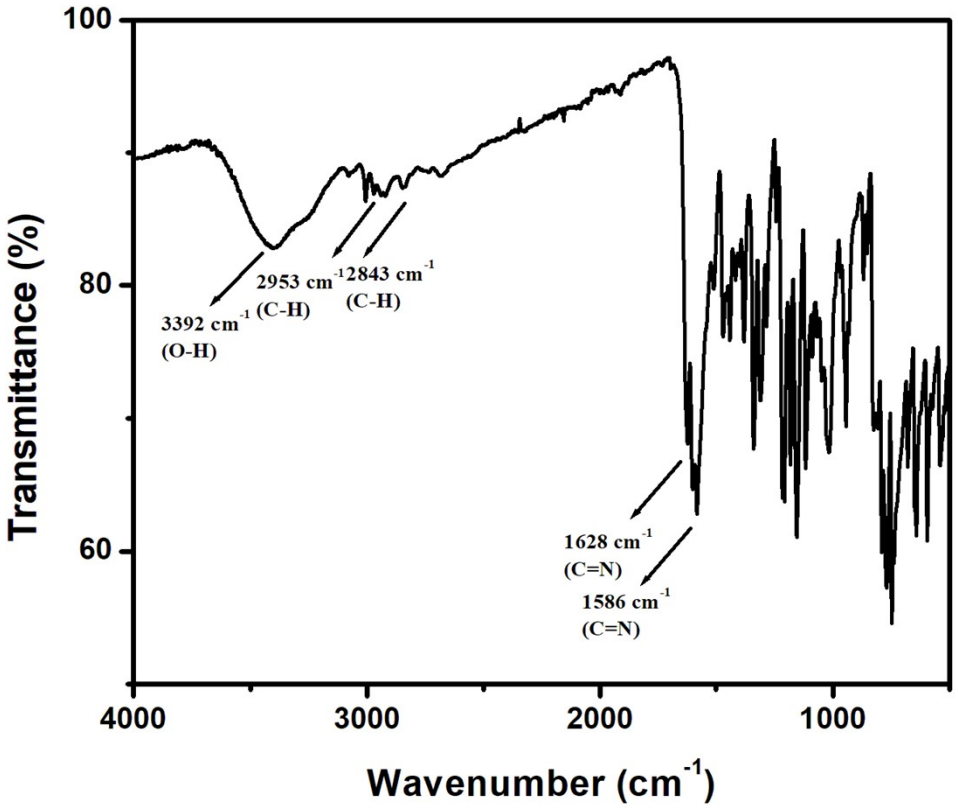

Fig.S4 IR Spectrum of the probe H_2L

Table S1. Crystal Data and Refined Parameters for H_2L

Empirical formula	**$C_{20}H_{18}N_2O_4$**
CCDC No.	2178275
Formula weight	350.36
Temperature (K)	100(2) K
System	Orthorhombic
Space group	P n a 21
a (Å)	11.7509(4)
b (Å)	9.3631(3)
c (Å)	30.1678(10)
α/°	90
β/°	90
γ/°	90
V (Å)^3	3319.21(19)
Z	8
D(cal) /g cm^{-3}	1.402
μ/mm^{-1}	0.813
λ(Å)	1.54178
Data[I >2σ(I)]/param	6304/474

R_1[a][I>2σ(I)]	0.0517
wR_2[b]	0.1343
GOF[c]	1.090

[a]$R_1 = \Sigma||F_o|-|F_c||/\Sigma|F_o|$; [b]$wR_2 = \{\Sigma[w(F_o^2-F_c^2)^2]/\Sigma[w(F^2_o)^2]\}^{1/2}$; $w = [\sigma^2(F_o)^2 + (0.1003P)^2 + 4.9693P]^{-1}$ $(F_o^2 + 2F_c^2)/3$; [c] Goodness-of-fit.

Table S2: Bond length of H_2L (Experimental & Theoretical):

Bond Length (Experimental)	**Å**	**Bond Length (Theoretical)**	**Å**
N2-N1	1.396	N12-N13	1.415
C22-N1	1.298	N12-C11	1.312
C22-C23	1.454	C11-C10	1.447
C23-C24	1.400	C10-C9	1.414
C24-O3	1.345	C9-O20	1.358
O3-H3	0.840	O20-H44	1.024
N2-C33	1.304	N13-C14	1.303
C33-C34	1.440	C14-C15	1.449
C34-C35	1.410	C15-C16	1.418
C35-O8	1.349	C16-O21	1.389
O8-H8	0.840	O21-H22	0.974

Table S3: Bond Angle of H_2L (Experimental and Theoretical):

Bond Angle (Experimental)	**Degree (°)**	**Bond Angle (Theoretical)**	**Degree (°)**
C33-N2-N1	112.45	C14-N13-N12	112.49

C22-N1-N2	113.91	C11-N12-N13	113.72
N1-C22-C23	120.65	N12- C11-C10	121.81
C22-C23-C24	119.92	C11-C10-C9	119.44
C23-C24-O3	123.07	C10-C9-O26	121.86
C24-O3-H3	109.50	C9-O20-H44	108.88
N2-C33-C34	131.96	N13-C14-C15	126.41
C33-C34-C35	122.12	C14-C15-C16	118.91
C34-C35-O8	121.31	C15-C16-O21	123.05
C35-O8-H8	103.42	C16-O21-H37	113.16

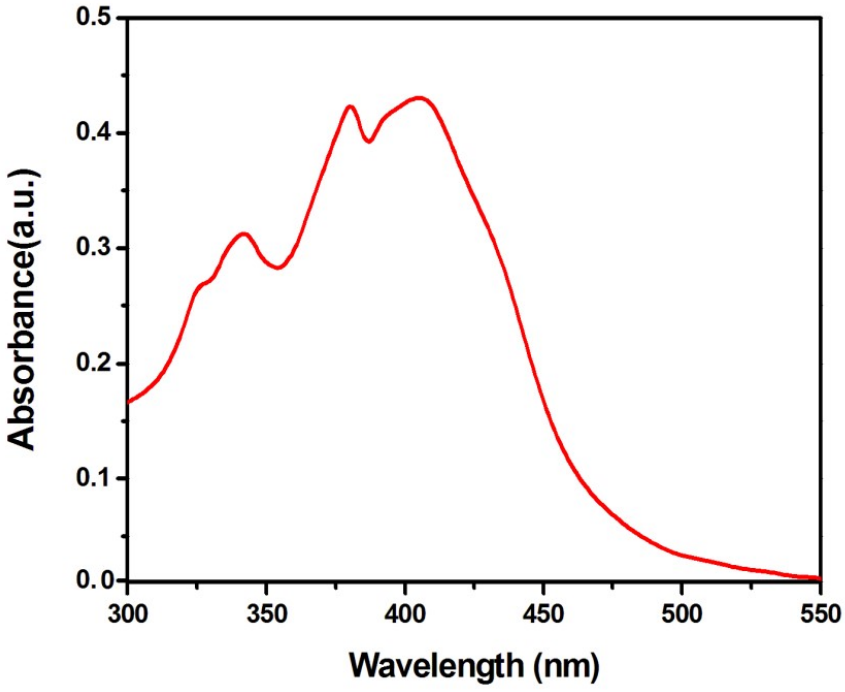

Fig.S5. Absorption Spectrum of H_2L in CH_3CN.

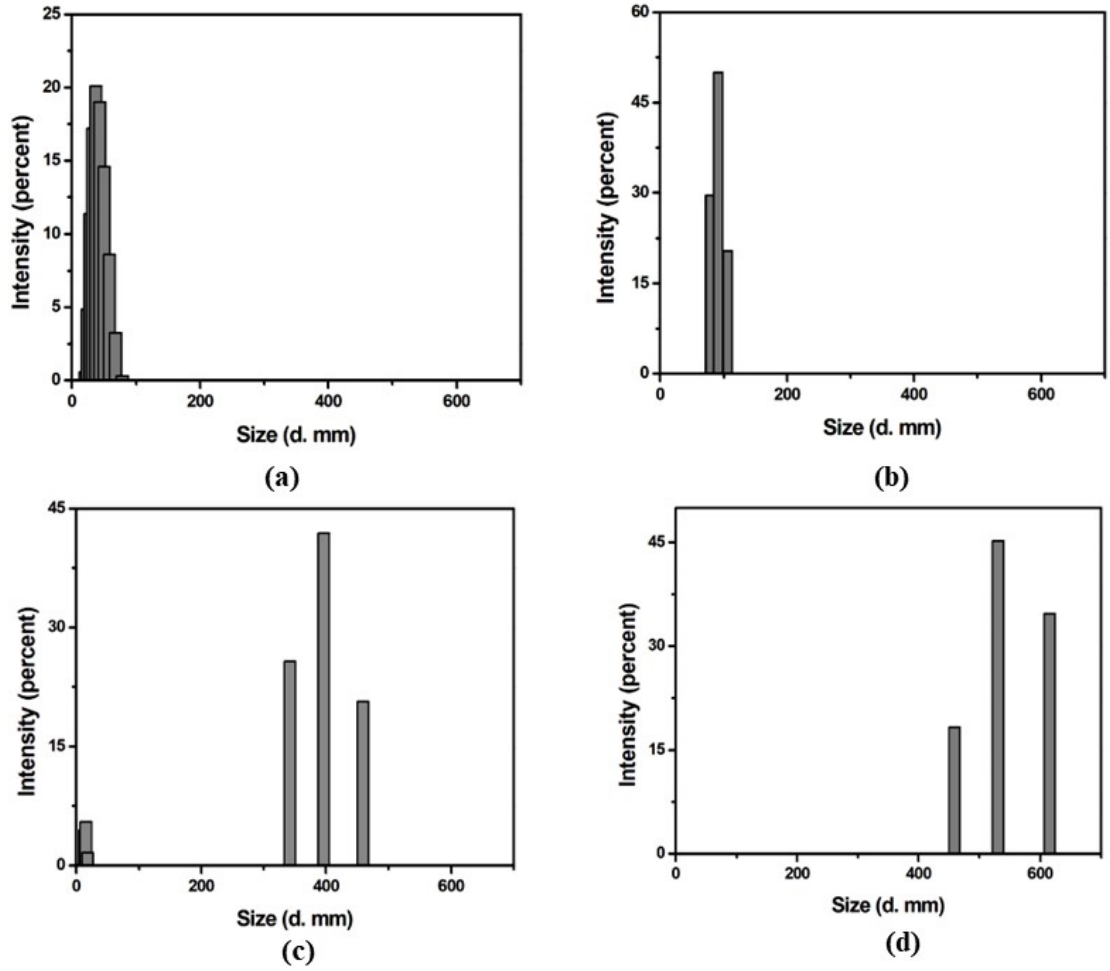

Fig.S6. DLS Spectrum of H_2L in CH_3CN/H_2O fraction f_w (a) 0% (b) 30% (c) 80% (d) 100%

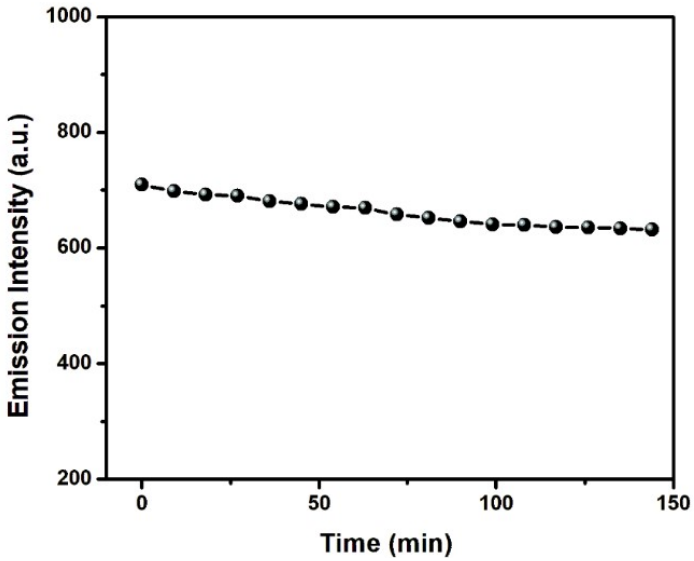

Fig.S7 Time-dependent fluorescence spectra of the thin film exposed to UV light (λ_{ex} = 365 nm) for 2.5 h

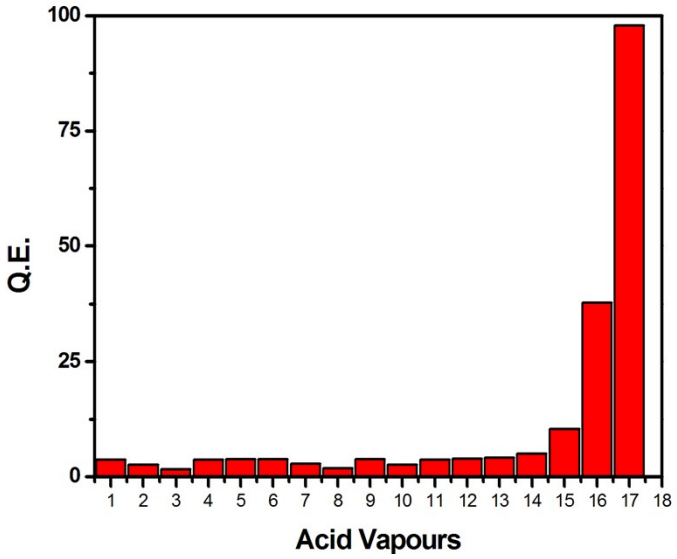

Fig. S8. Bar plot showing QE(%)s of solid emissive test kits after exposure to the saturated acid vapors of common interfering agents for 10 minutes. The analytes used are: 1. Acetonitrile (CH_3CN) 2. Ethanol (EtOH) 3. Tetrahydrofuran (THF) 4. Dichloromethane (DCM) 5.n-Hexane (n-HXN) 6. Toluene (TOL) 7. phosphoric acid, 8. propionic acid, 9. sulphuric acid, 10. methane sulfonic acid, 11. methacrylic acid, 12. heptanoic acid, 13. oleic acid, 14. Acetic Acid (AcOH) 15. Nitric Acid (HNO_3) 16. Hydrochloric Acid (HCl) and 17. Trifluoroacetic Acid (HTFA). The emission was recorded with 5 minutes interval for each turn.

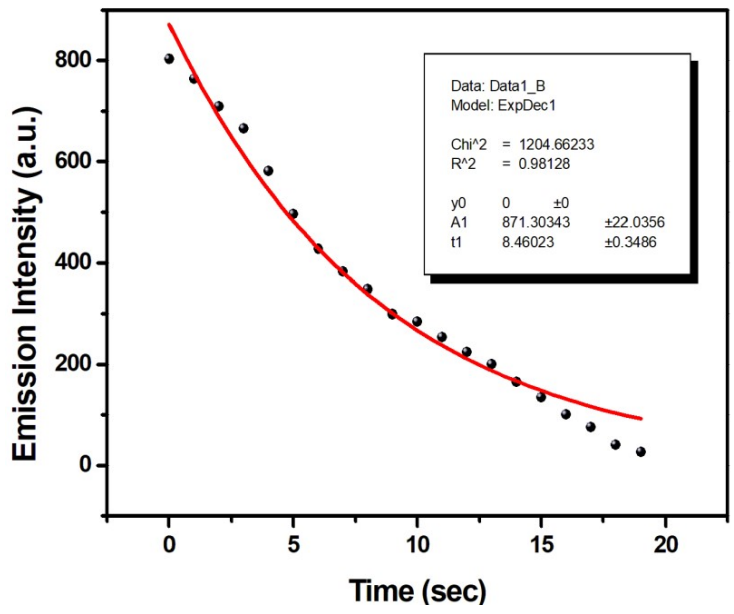

Fig. S9. Kinetics of time dependent response Decay

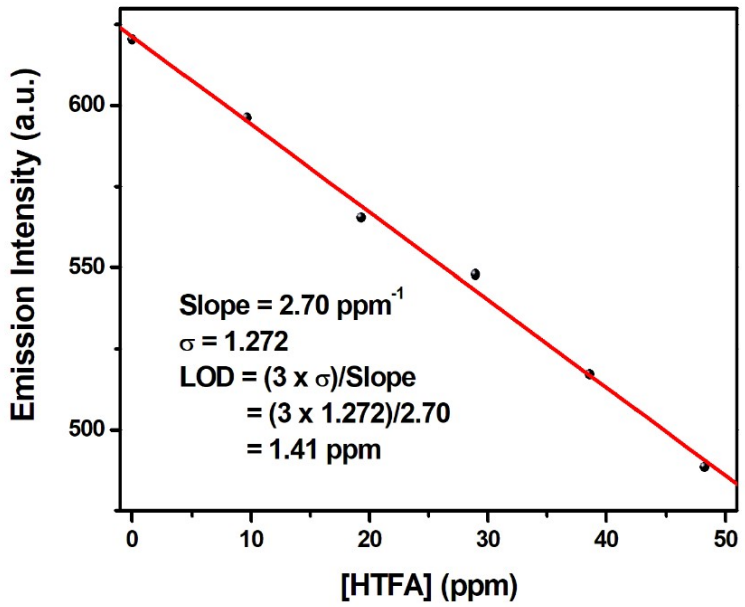

Fig. S10. Limit of Detection for HTFA Vapor Sensing.

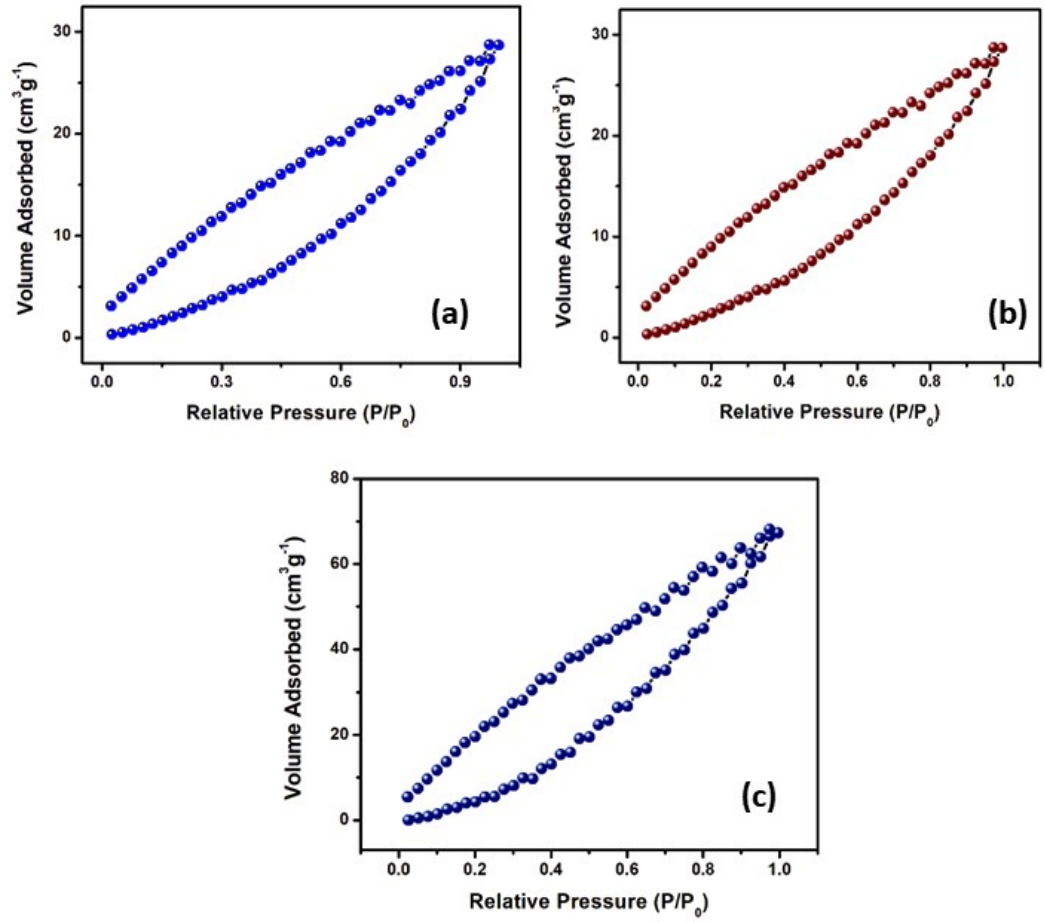

Fig.S11. Nitrogen adsorption–desorption isotherms of (a) H_2L, (b) H_2L+HTFA and (c) H_2L+HTFA+TEA.

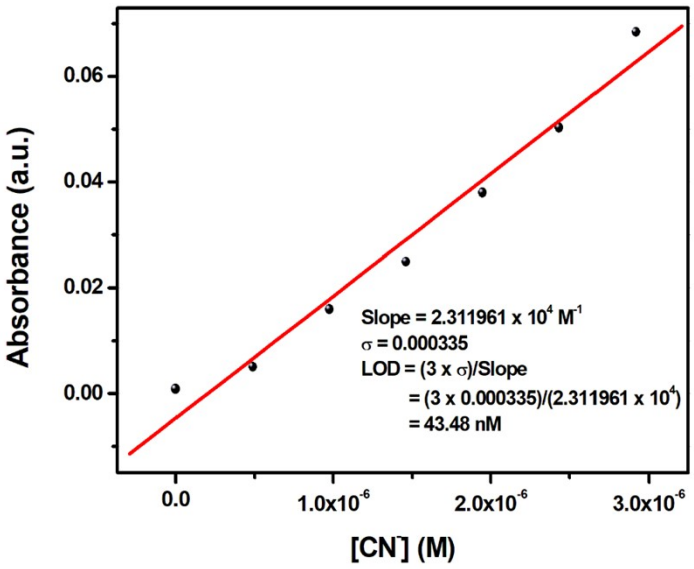

Fig. S12. Limit of Detection for CN^- sensing of the probe H_2L.

Table S4: Comparative Table for Reported Probes towards CN^- and TFA detection and their sensing features.

Sl. No.	**Reported Probes**	**Selectivity/ Sensing Solvent/ Stability**	**Sensing Mechanism**	**Sensing Method (Dual Channel)/ LOD (Sensitivity)**	**Ratio-metric Response/ Dual Response**	**Real Applications in environment-al, food and biological samples/ Test Strip** or Thin film	**Logic gate circuit/ Bioima-ging in plants and animals**	**Ref.**
1.	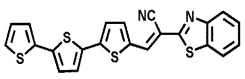	CN^-/ DMSO:H_2O (9:1, v/v)	Nucleophilic addition to C=C bond, Intramolecular	Fluorometric [Turn On] Colorimetric	No/ No	Yes (Food Extract)/ Yes	No/ Yes	[1]

			Charge Transfer (ICT)	(Yes)/ 0.46 μM				
2.	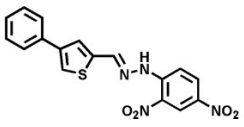	CN^-/ $CH_3CN:H_2O$ (7:3, v/v)	ILCT (Intra ligand Charge Transfer) followed by Deprotonation of NH proton	Colorimetric (No)/ 46.2 nM	No/ No	Yes (Food extract & water sample)/ No	No/ No	[2]
3.	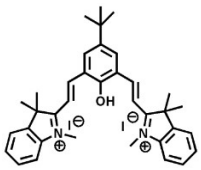	CN^-/ DMSO/Yes	Nucleophilic addition to C=N bond, ICT	Fluorometric [Turn On] Colorimetric (Yes)/ 21 nM	No/ No	Yes (Food Extract)/ No	No/ No	[3]
4.	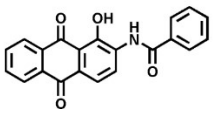	CN^-/ $CH_3CN:H_2O$ (95:5, v/v)	Deprotonation of O-H proton	Colorimetric (No)/ 0.22 μM	No/ No	No/ Yes	No/ No	[4]
5.	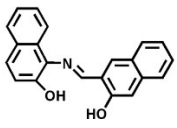	CN^- /DMF:H_2O (1:1, v/v)/ Yes	Deprotonation of O-H proton and Nucleophilic addition to C=N bond	Fluorometric [Turn OFF] Colorimetric (Yes)/ 0.21 μM	No/ No	No/ No	No/ Yes	[5]
6.								

	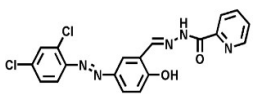	CN^-/ DMSO:H_2O (6:4, v/v)	Deprotonation of O-H and N-H proton	Colorimetric (No)/ 6.4 μM	No/ No	No/ Yes	No/ No	[6]
7.	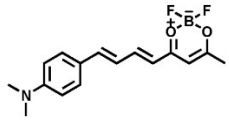	CN^-/ THF:H_2O (8:2)/ Yes	CN^- addition to C=C double bond	Fluorometric [Turn ON] Colorimetric (Yes)/ 2.23 μM	No/ No	Yes (Food and Water Analysis)/ No	No/ Yes	[7]
8.	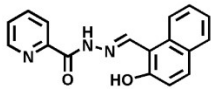	CN^-/ DMSO:H_2O (9:1, v/v)	Deprotonation of O-H proton	Colorimetric (No)/7.08 μM	No/ No	No/ Yes	No/ No	[8]
9.	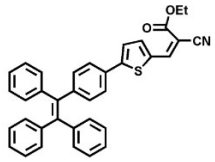	CN^-/ DMSO	Nucleophilic addition to C=C bond, ICT	Fluorometric [Turn OFF] Colorimetric (Yes)/ 67 nM	No/ No	Yes (Food Extract)/ Yes	No/ Yes	[9]
10.	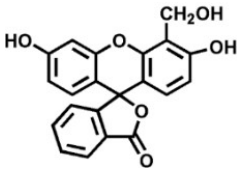	CN^-/ CH_3CN/ Yes	Deprotonation of O-H and COOH, ICT	Colorimetric (No)/3.68 μM	No/ No	No/ No	No/ No	[10]
11.	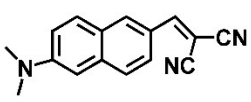	CN^-/ DMSO/H_2O (6:4, v/v)	Nucleophilic addition to C=C bond, ICT	Fluorometric [Turn ON] Colorimetric	Yes/ No	No/ No	No/ No	[11]

				(Yes)/ 0.18 μM.				
12.	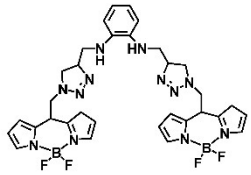	CN^-, F^-/ THF	Deprotonation of C-H proton	Colorimetric (No)/ 72 (CN^-) and 83 nM (F^-)	No/ Yes	No/ No	No/ No	[12]
13.	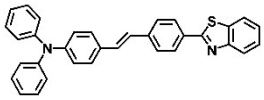	HTFA HNO_3, HCl/ $CHCl_3$ Solid-state (Solvent free)	Protonation of N donor of benzothiazole moiety, ICT	Fluorometric [Turn OFF] Colorimetric (Yes)/ 2.8 ppm (TFA)	No/ No	No/ Yes	No/ No	[13]
14.	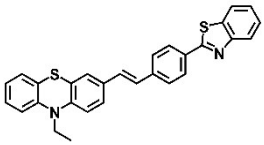	HTFA, HNO_3 HCl/ CH_3Cl_3/Yes	Proronation of N donor benzothiazole moiety, ICT	Fluorometric [Turn OFF] Colorimetric (Yes)/ 2.3 ppm (TFA)	No/ No	No/ Yes	No/ No	[14]
15.	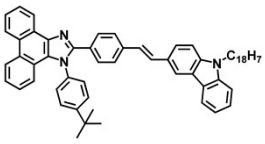	HTFA/ CH_2Cl Solid-state (Solvent free)	Protonation of Imidazole moiety, ICT	Fluorometric [Turn ON] (No)/ 7.4 ppm	Yes/ No	No/ Yes	No/ No	[15]

16.

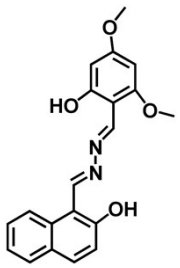	HTFA, CN^-/ Solid-State (HTFA Vapour)/Yes CH_3CN/H_2O (99:1, v/v) (CN^-)/Yes	Protonation of the imine N of the azine derivative (TFA) Deprotonation of O-H (CN^-)	Fluorometric [Turn OFF-TFA] [Turn ON-CN^-] Colorimetric [TFA, CN^-] (Yes)/ 1.41 ppm (TFA) 45.42 nM (CN^-)		No/ Yes	Yes (Food Extract) (CN^-)/ Yes (CN^-/HTFA)	Yes (CN^-)/ Yes (CN^- /AIE)	This work

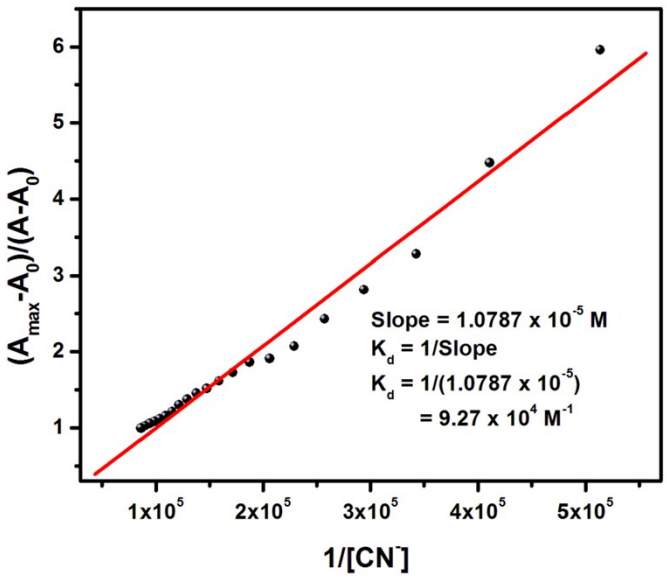

Fig. S13. Determination of Binding Constant (K_d) from from Benesi-Hildreband Plot of CN^- Titration Curve.

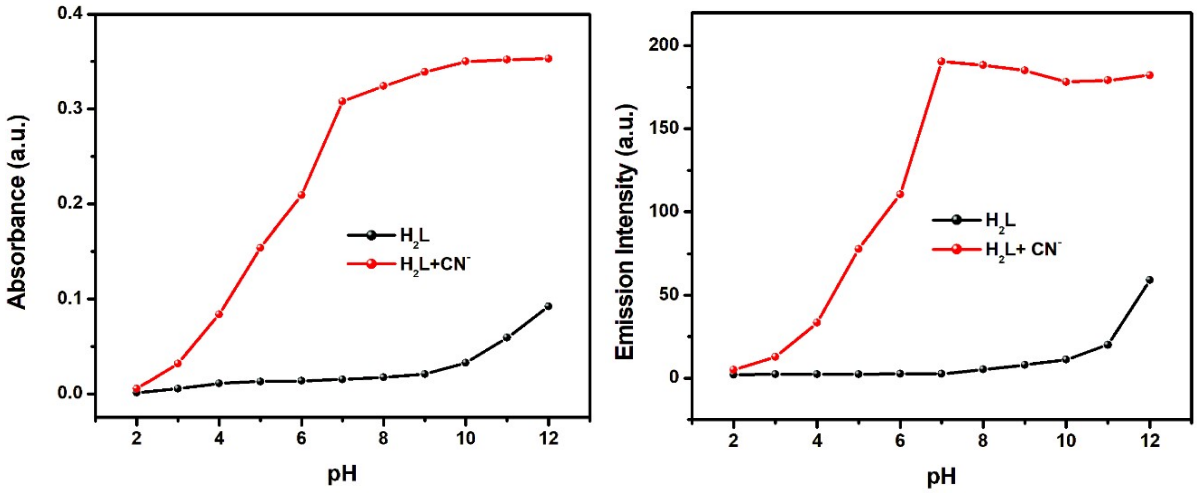

Fig.S14. Changes in **(a)** Absorption (λ_{abs} = 479 nm) and **(b)** Emission Spectra (λ_{exc} = 570 nm) of H_2L and H_2L+CN under different pH.

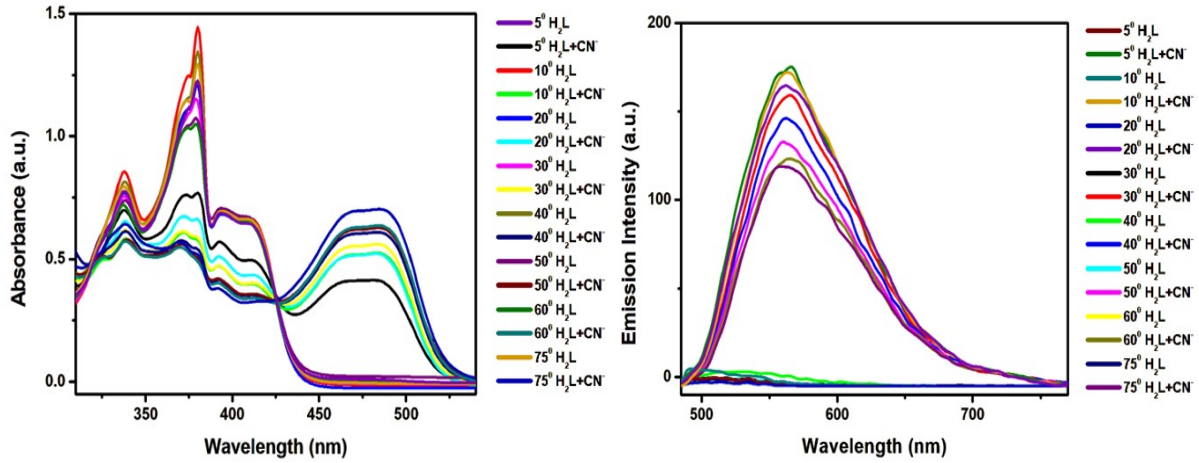

Fig.S15. Changes in **(a)** Absorption (λ_{abs} = 479 nm) and **(b)** Emission Spectra (λ_{exc} = 570 nm) of H_2L and H_2L+CN^- under temperature variation from 5°C to 75°C.

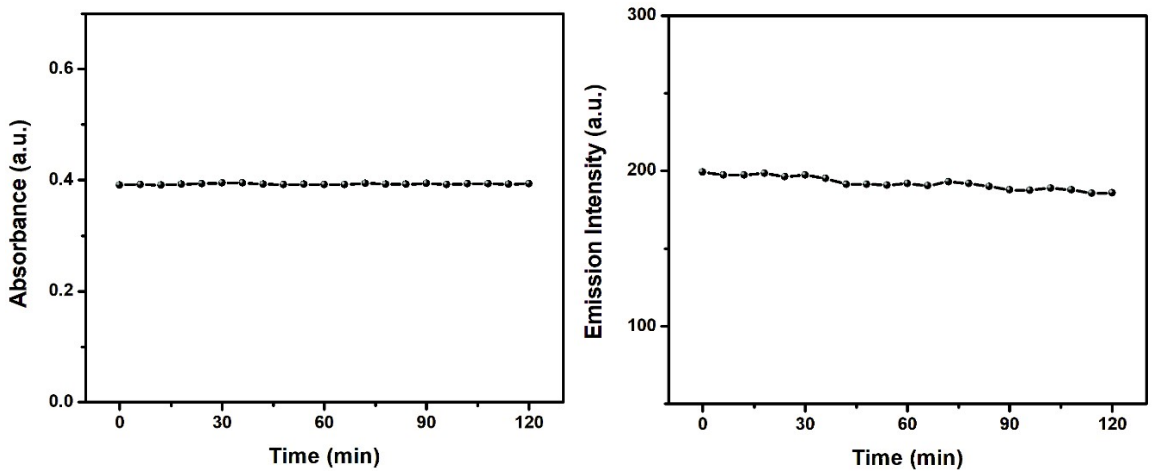

Fig.S16. Changes in **(a)** Absorption (λ_{abs} = 479 nm) and **(b)** Emission Spectra (λ_{exc} = 570 nm) of H_2L and H_2L+CN^- on time variation for about 2 hrs.

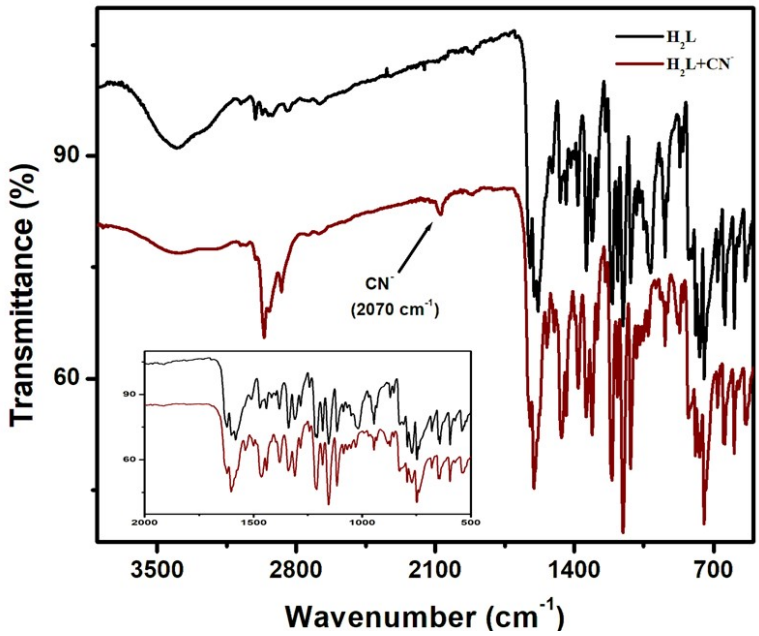

Fig.17. IR spectrum of H_2L and (H_2L+CN^-) adduct (Inset: Expanded Region from 2000 cm^{-1} to 500 cm^{-1}.

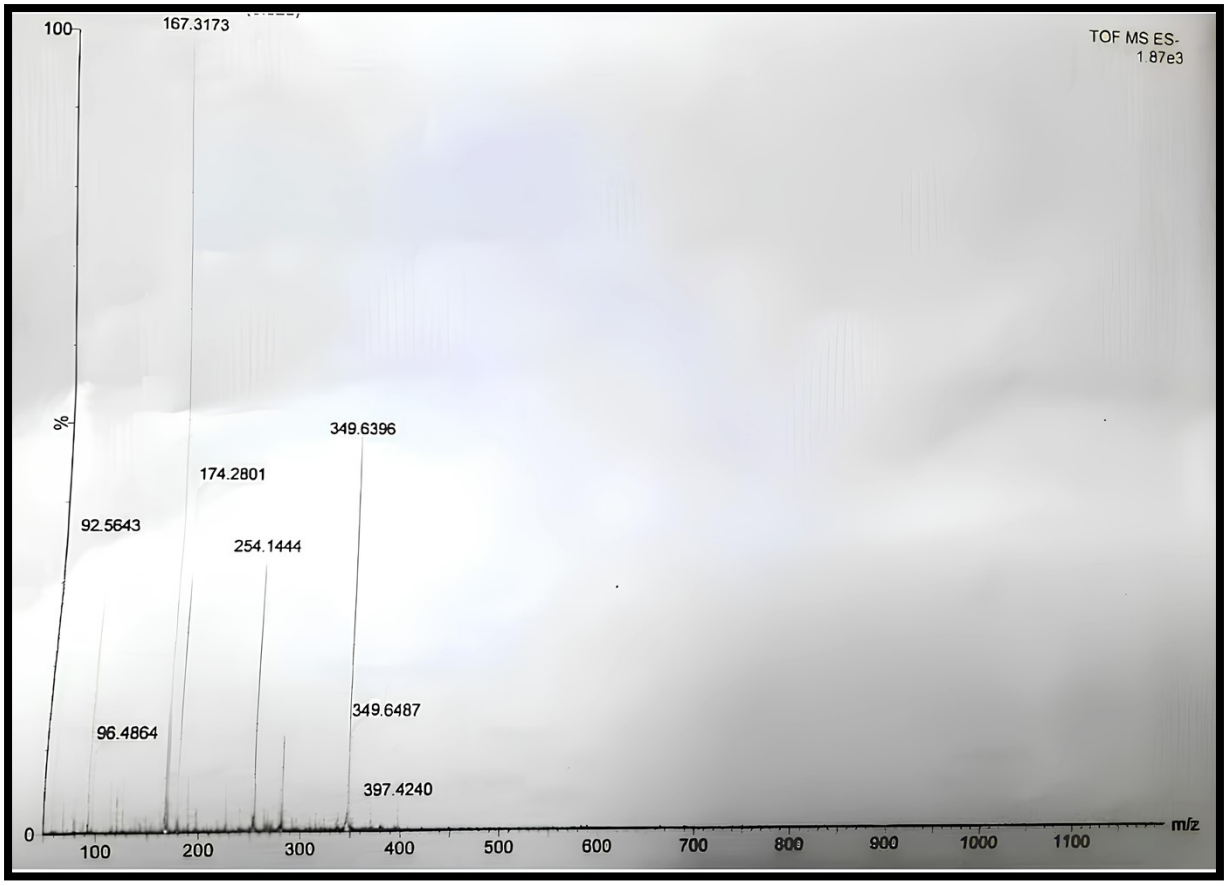

Fig. S18. ESI-MS (-ve) mode of CN^- Complex (H_2L+2CN^-)

Table S5: TD-DFT transition of H_2L and CN^- complex (L^{2-}) .

System	Vertical Excitation Energy (eV)	Exp. Wavelength (nm)	Theor. Wavelength (nm)	Oscillation Frequency	Key Transition
H_2L	3.1252	410	409.04	1.0918	HOMO →LUMO
	3.7225	337	334.15	0.1548	HOMO-2 →LUMO
L^{2-}	2.7410	474	452.33	0.8995	HOMO →LUMO
	3.9154	338	316.66	0.0283	HOMO-1→LUMO+1

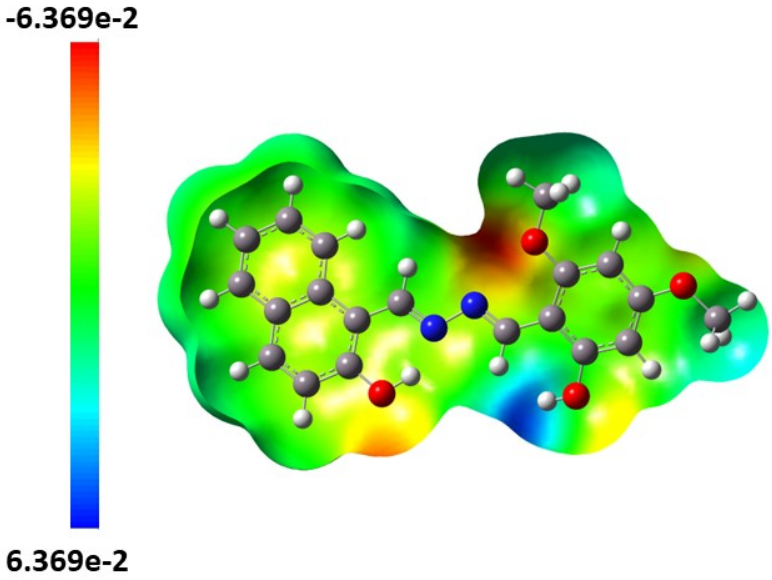

Fig.S19. Electrostatic Potential (ESP) Mapping of the optimized probe H_2L calculated from B3LYP/6-311g level with scale bar (Kcal/mol).

Table S6: Orbitals of H_2L and their corresponding energies.

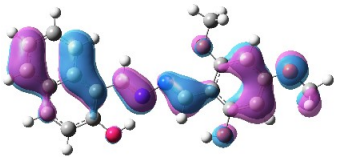	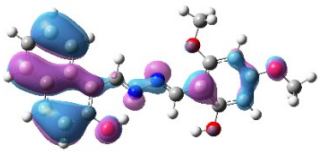	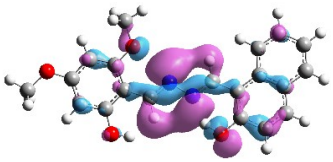
HOMO-5 (-7.36 eV)	HOMO-4 (-6.36 eV)	HOMO-3 (-6.33 eV)
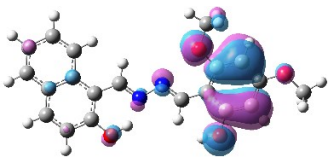	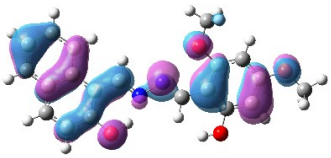	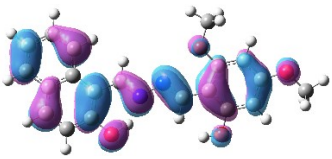
HOMO-2 (-6.19 eV)	**HOMO-1 (-6.15 eV)**	**HOMO (-5.37 eV)**

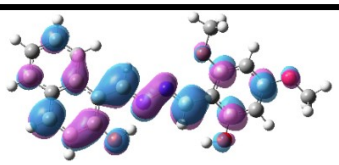

LUMO

(-1.97 eV)

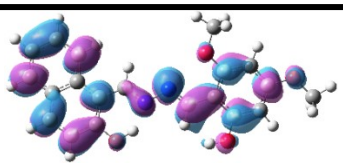

LUMO+1

(-0.90 eV)

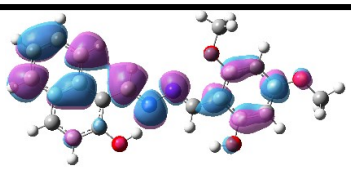

LUMO-+2

(-0.10 eV)

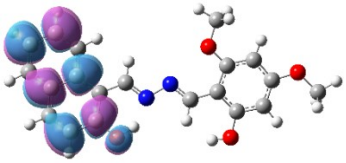

LUMO+3

(-0.02 eV)

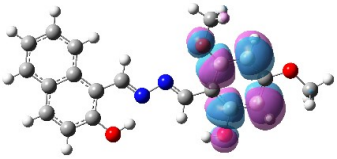

LUMO+4

(0.23 eV)

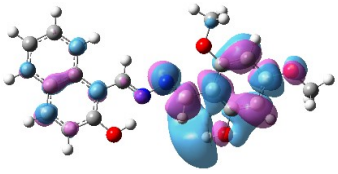

LUMO+5

(1.25 eV)

Table S7: Molecular Orbitals of L^{2-} and their corresponding energies.

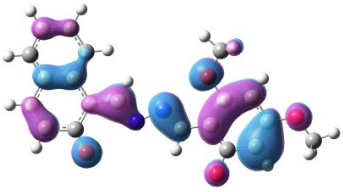

HOMO-5

(0.01 eV)

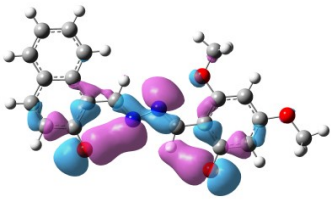

HOMO-4

(0.15 eV)

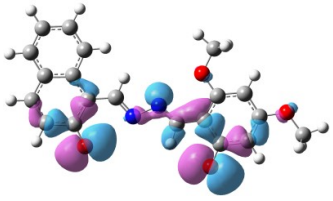

HOMO-3

(0.41 eV)

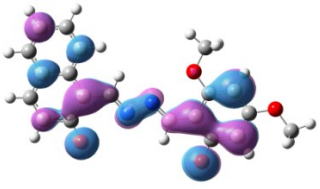

HOMO-2

(0.93 eV)

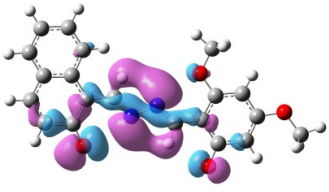

HOMO-1

(1.02 eV)

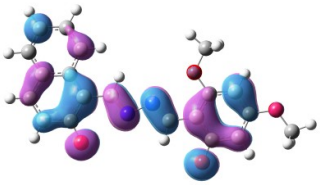

HOMO

(1.61 eV)

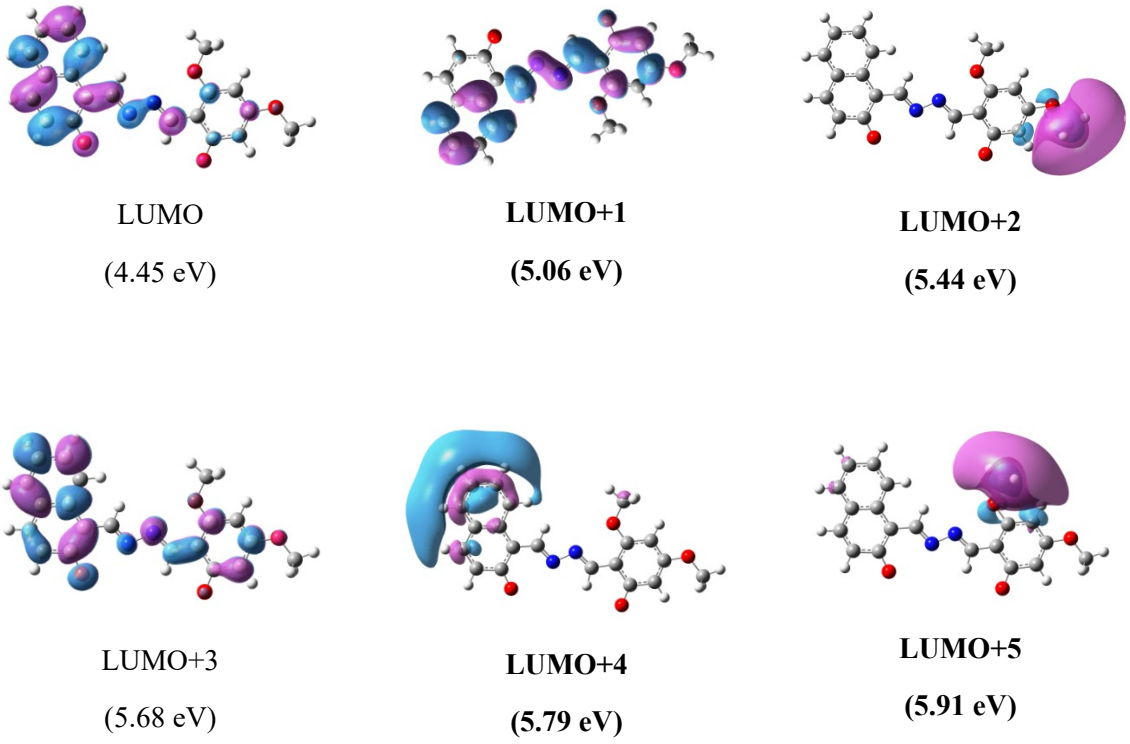

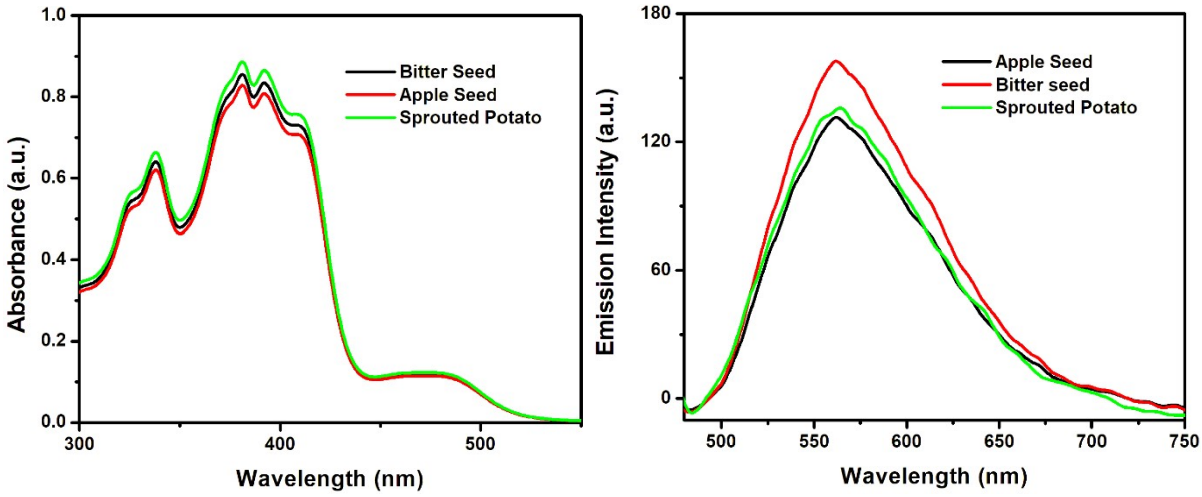

Fig.S20. (a) Absorption and (b) Fluorescence Spectra of H_2L towards CN^- in different food samples.

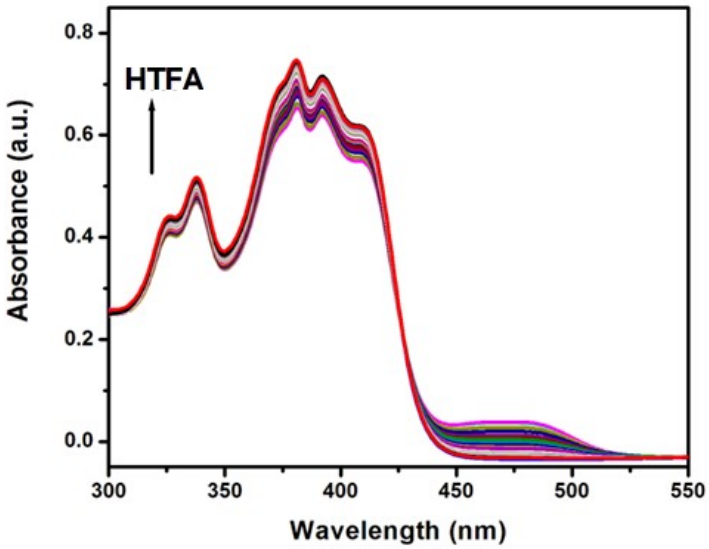

Fig.S21. Change in Absorption Spectra of CN^- Complex on gradual addition of HTFA (H^+).

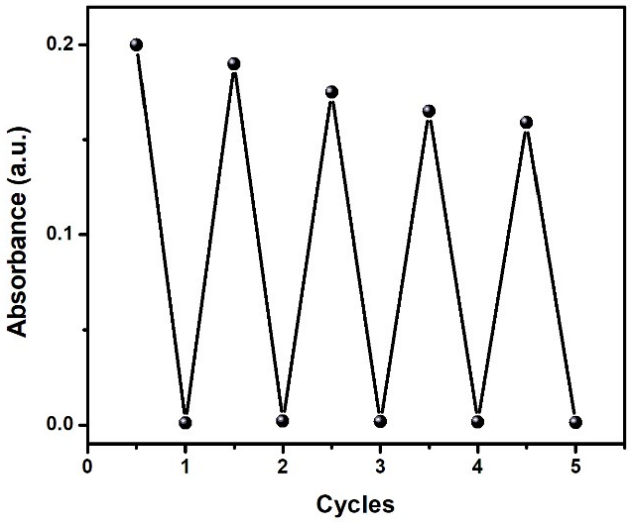

Fig.22. Reversible Cycles on addition of CN^-/HTFA.

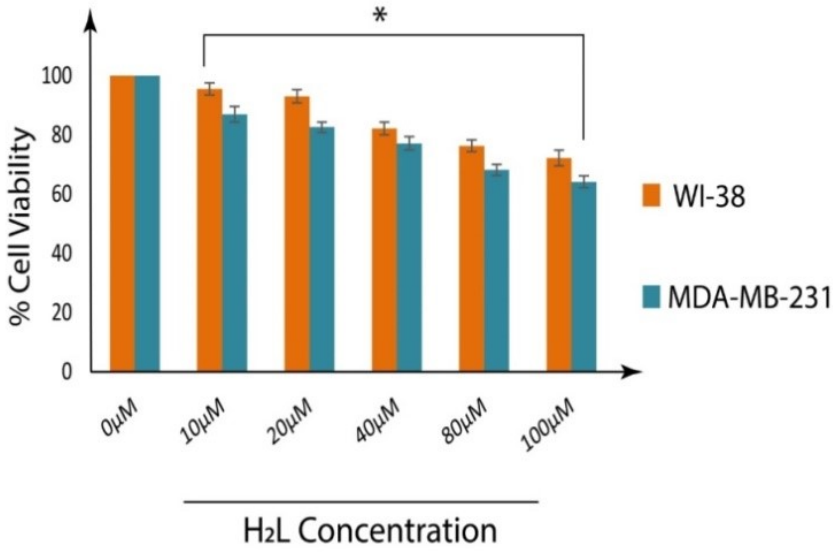

Fig. S23. Cell survivability of MDA-MB 231 and WI-38 cells exposed to ligand H_2L concentration. Data are representative of at least three independent experiments and bar graph shows mean ± SEM, $*p < 0.001$ were interpreted as statistically significant, as compared with the control

Reference:

1. Q. Niu, L. Lan, T. Li, Z. Guo, T. Jiang, Z. Zhao, Z. Feng, J. Xi, *Sens. Actuators B Chem.,* 2018, **276**, 13-22

2. P. Karuppusamy, S. Sarveswari, *J. Mol. Struct.,* 2022, **1248**, 131494.

3. R. Shanmugapriya, P. Saravana Kumar, S. Ponkarpagam, C. Nandhini, K.N. Vennila , A. G. Al-Sehemi, M. Pannipara, K. P. Elango, *J. Mol. Struct.,* 2022, **1251**, 132081.

4. T. P. Martyanov, A. A. Kudrevatykh, E. N. Ushakov, D.V. Korchagin, I. V. Sulimenkov, S. G. Vasil'ev, S. P. Gromov , L. S. Klimenko, *Tetrahedron,* 2021, **93**, 132312.

5. B. Yilmaz, M. Keskinates, Z. Aydin, M. Bayrakci, *J. Photochem. & Photobio. A: Chem.,* 2022, **424**, 113651

6. Z. Li, C. Liu, S. Wang, L. Xiao, X. Jing, *Spectrochim. Acta A,* 2019, **210**, 321–328.

7. Y. Gao, M. Li, X. Tian, K.Xu, S.Gong, Y. Zhang, Y.Yang, Z. Wang, S. Wang, *Spectrochim. Acta A,* 2022, **271**, 120882.

8. S. Dey, C. Sen, C. Sinha, *Spectrochim.Acta Part A.,*2020, **225**, 117471.

9. G.A. Zalmi, D.N. Nadimetla, P. Kotharkar, A. L. Puyad, M. Kowshik, and S. V. Bhosale, *ACS Omega* 2021, **6**, 16704−16713.

10. R. V. Rathod, S. Bera, D. Mondal, *Spectrochim. Acta A*, 2020, **238**, 118419.

11. J.-J. Li, W. Wei, X.-L. Qi, X. Xu, Y.-C. Liu, Q.-H. Lin, W. Dong, *Spectrochim.Acta Part A.,* 2016*,* **152***,* 288-293.

12. W. Saiyasombat, U. Eiamprasert, T. Chantarojsiri, K. Chainok, S. Kiatisevi, *Dyes Pigments,* 2022, **206**, 110643.

13. Y. Zhan, P. Yang, G. Li , Y. Zhang and Y. Bao, *New J. Chem.*, 2017, **41**, 263-270.

14. Y. Zhan, J. Zhao, P. Yanga and W. Ye, *RSC Adv.*, 2016,**6**, 92144-92151

15. J. Peng, J. Sun, P. Gong, P. Xue, Z. Zhang, G. Zhang, R. Lu, *Chem. Asian J.*, 2015, **10**, 1717-1734.